NUMERICAL HYDRODYNAMIC CALCULATIONS OF CATHETER CHARACTERISTICS

W. W. AKERS, A. C. L. BARNARD, H. M. BOURLAND,
W. A. HUNT, W. P. TIMLAKE, *and* E. VARLEY
From the IBM Scientific Center and the Bio-Medical Laboratories, Rice University, Houston, Texas

ABSTRACT The theory of fluid flow in compliant tubes developed in a previous paper is applied to a catheter, and the results of various calculations are compared with experiment. When a parabola is used for the unknown velocity profile, the calculated gains are too high. Agreement is slightly improved by using more reasonable profiles. It is shown that there exists a functional relationship between the parameter γ and the nondimensional parameter α_w which gives reasonable agreements with all the experimental data considered. The theory of Womersley is applied to the catheter, and the calculated gains are larger than those observed experimentally. A form for the frictional force suggested by Lambossy is used in some further calculations.

INTRODUCTION

Although catheter tip pressure transducers are becoming more common, the practice of measuring pressure pulses at the distal end of a long catheter is still widespread. In propagating down a long catheter, the pressure pulse will, in general, be changed in form and the characteristics of the catheter must be known in order to deduce the pressure variation at the proximal end from that measured at the distal end. Akers and Bourland have recently measured the characteristics of catheters experimentally, using sinusoidally varying driving pressures of variable frequency. At each frequency, proximal and distal pressures were measured to obtain the gain of the catheter. The present paper attempts to reproduce these results theoretically, using the approach outlined in the previous paper (1), which will be referred to as I.

EXPERIMENTAL RESULTS

The measurements of Akers and Bourland (personal communication) appear as solid dots on Figs. 1 and 2. Staham P23DB pressure transducers were used. The quantity plotted, "gain," is the distal amplitude divided by the proximal amplitude, the amplitudes being obtained from strip-chart records of the experiments. The

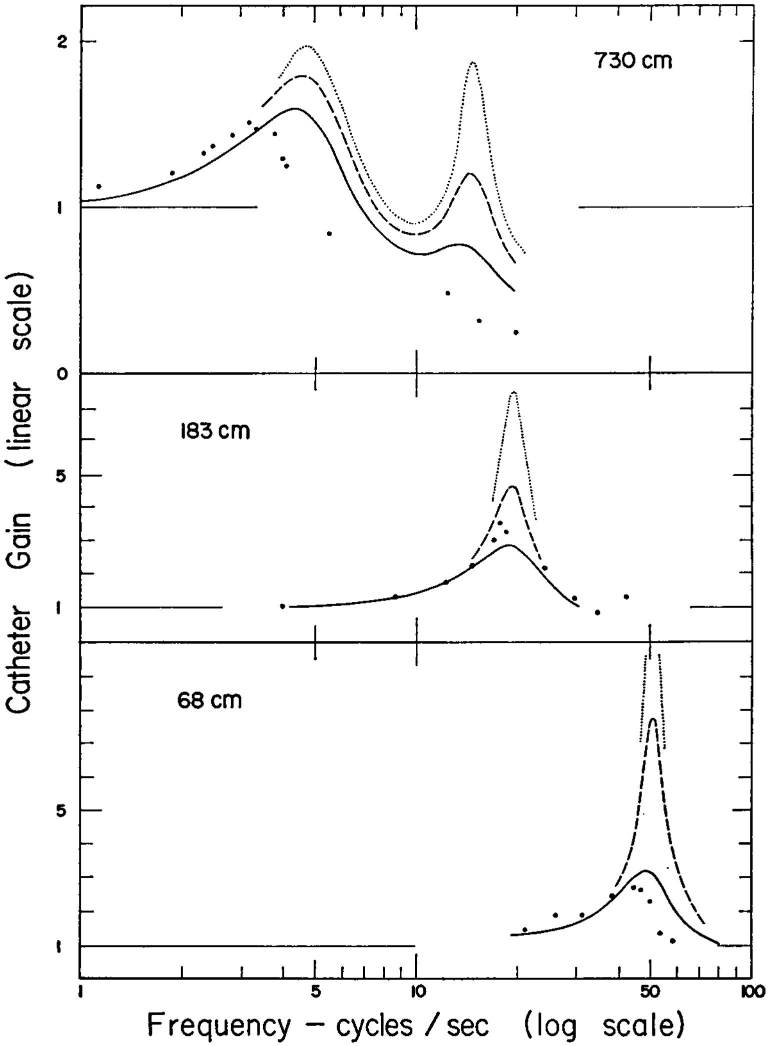

FIGURE 1 Gain as a function of frequency for polyethylene catheters of different lengths L. The dots are the experimental points, and the solid, dashed, and dotted curves are calculated as described in the text. Upper $L = 730$ cm; middle $L = 183$ cm; and lower $L = 68$ cm.

experimental measurements were made for two catheter materials, polyethylene and silastic rubber, and extended over a wide range of frequencies and catheter lengths. The polyethylene and silastic catheters had different diameters. In static measurements to determine the wall elasticity, a known volume of liquid was injected into the catheter and the resulting pressure was measured. The quantity of liquid flowing per second under a steady pressure gradient was also measured.

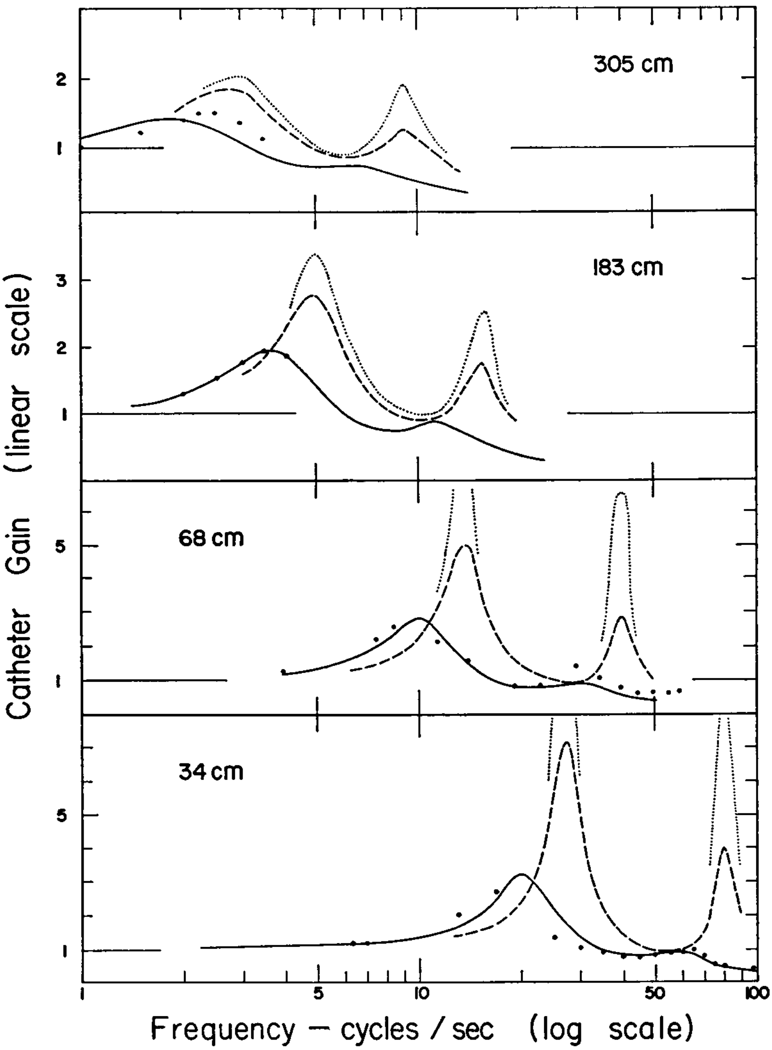

FIGURE 2 Results for silastic rubber catheters. See caption to Fig. 1. Upper $L = 305$ cm; upper middle $L = 183$ cm; lower middle $L = 68$ cm; and lower $L = 34$ cm.

While the experiments were in progress, it was noticed that the presence of a small air bubble in the catheter drastically changed its characteristics. In an attempt to remove such bubbles, the catheters were flushed out with carbon dioxide before measurements were made. However the possible presence of extremely small bubbles remains a source of uncertainty in the measurements. The effect of bubbles is to reduce the gain at resonance and shift the resonance to lower frequencies.

CALCULATIONS

The velocities and pressures were initially set to zero throughout the catheter and the proximal driving pressure was taken to have the form $P = P_o$ (1-cos ωt). At the distal end ($z = L$) the boundary condition (see I)

$$U_{\text{distal}} = (k_t/A)(\partial P/\partial t)_{\text{distal}}$$

with

$$\frac{\partial P}{\partial t} \doteq \frac{P(t, L) - P(t - \Delta t, L)}{\Delta t}$$

was applied. k_t is known from the properties of the pressure transducer (for applied pressure P the volume displacement of the transducer is $k_t P$). The proximal pressure and velocities, and the distal pressures, were the output from the calculation. The calculations were continued for several cycles, until the distal pressure had settled into a sinusoidal form with a well defined amplitude. This method of calculation also gives the absolute phase relationship between the proximal and distal pressures. The input quantities are listed in Tables I and II; a sample of the output is shown in Fig. 3.

The first calculations were made using the parabolic velocity profile discussed in I, in which case the parameter γ is constant and equal to 8 $\pi\nu$, where ν is the

TABLE I

INPUT QUANTITIES FOR POLYETHYLENE CATHETERS (CGS UNITS)

$\alpha = 1.33$* (dimensionless)	Alpha parameter
$\gamma = 0.251$* (cm^2/sec)	Gamma parameter
$k = 1.83 \times 10^{10}$ dyne/cm^4	Pressure-area relation ($p = k\Delta A$)
$A_0 = 0.12$ cm^2	Unstressed cross-section
$\beta = 10^5$ dynes/cm^2	Amplitude of sinusoidal driving pressure
$k_t = 3 \times 10^{-10}$ cm^5/dyne	Transducer characteristic

* Used to calculate dotted curve on Fig. 1.

TABLE II

INPUT QUANTITIES FOR SILASTIC RUBBER CATHETERS (CGS UNITS)

$\alpha = 1.33$*	(dimensionless)
$\gamma = 0.251$*	cm^2/sec
$k = 6.44 \times 10^8$	dyne/cm^4
$= 3\ 6 \times 10^8$‡	dyne/cm^4
$A_0 = 0.0211$	cm^2
$\beta = 10^5$	dynes/cm^2
$k_t = 3 \times 10^{-10}$	cm^5/dyne

* Used to calculate dotted curve on Fig. 2.
‡ Used to calculate solid curve on Fig. 2.

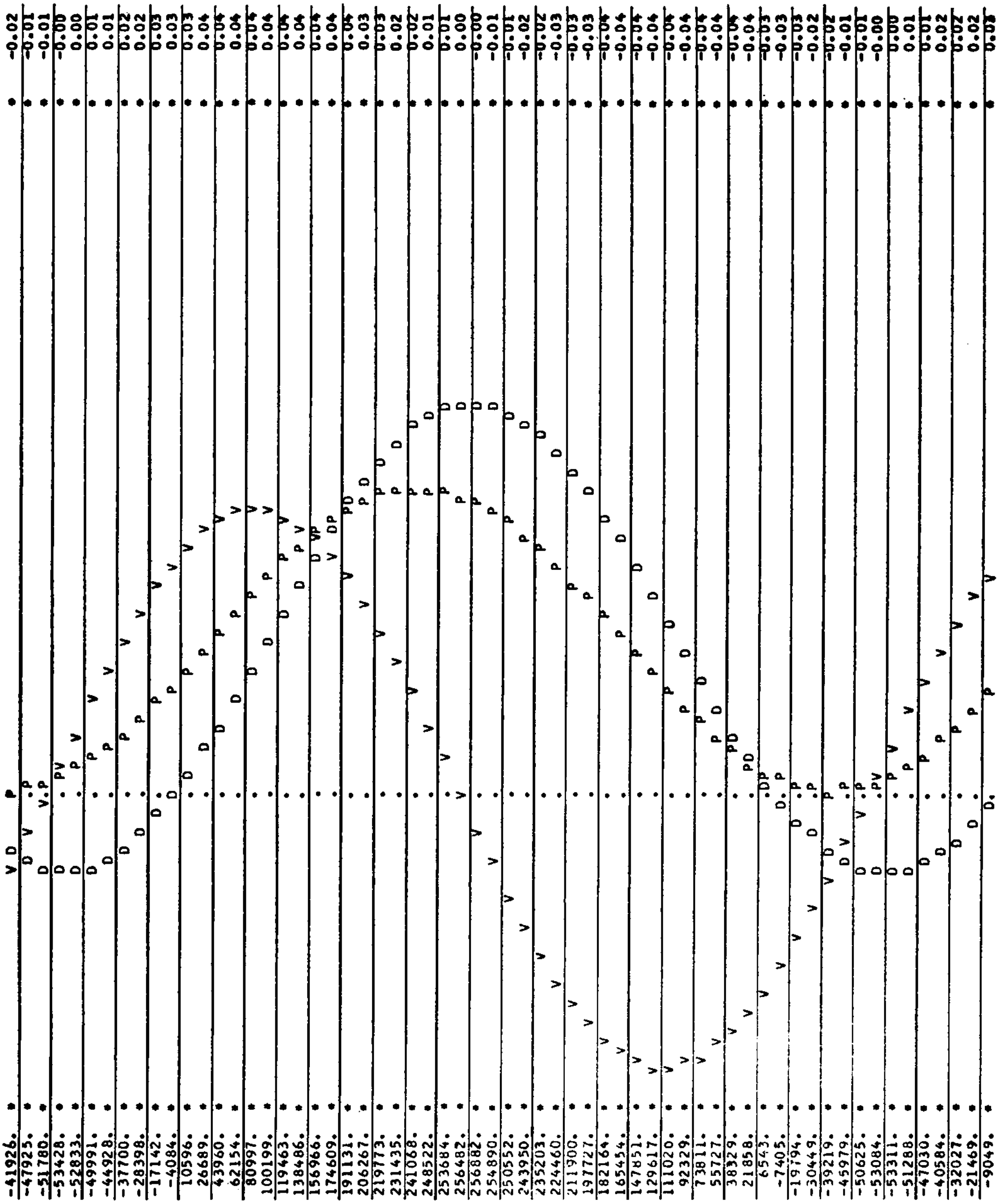

FIGURE 3 Sample output from calculation. The time axis runs from left to right. Letters *P*, *D*, and *V* form graphs of the proximal and distal pressures and the proximal velocity, respectively. The numbers at the bottom are the distal pressures and at the top are the distal velocities.

kinematic viscosity. Then $\gamma = 0.25$ cm^2/sec which is in good agreement with the value of 0.28 obtained from the steady flow data. Although the results were qualitatively correct, the gains were too large, as can be seen from the dotted curves in Figs. 1 and 2. This indicates that the actual system is considerably more damped than the mathematical model with this profile.

Calculations of velocity profiles in rigid tubes by Womersley (2) and Lambossy (3) indicate that the profile is not parabolic except at low values of the dimensionless parameter $\alpha_w = R(\omega/\nu)^{1/2}$ where ω is the angular frequency of the sinusoidal driving pressure and R is the tube radius. At higher values of α_w the profile is neither parabolic nor constant through the cycle and it is not possible to relate $(\partial v_z/\partial r)_R$ to U in a simple way. In this case the parameter γ varies through the cycle with typical values larger than those obtained with the parabolic profile. This corresponds to a more damped system.

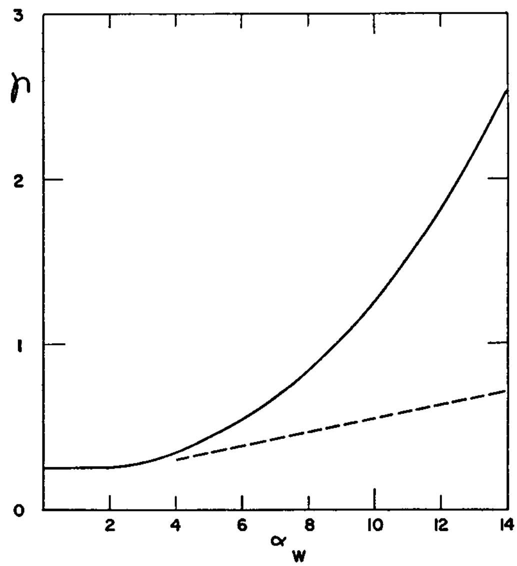

FIGURE 4 Values of the parameter γ as a function of the nondimensional parameter α_w. The dashed curve was estimated as described in the ext and was used to calculate the dashed curves on Figs. 1 and 2. The solid curve represents values adjusted to fit the data, i.e., to calculate the solid curve on Figs. 1 and 2.

It would appear possible to estimate an "effective" constant value of the parameter by using the approximate profile calculations and taking the value of γ at the instant the flow is maximal. The values of γ obtained in this way are shown as a function of α_w in Fig. 4. The calculations were repeated using this method of estimating γ, with the improved results shown as dashed curves in Figs. 1 and 2.

At this stage it should be emphasized that thus far the calculation has been made without adjusting parameters to fit the data. The value of the parameter γ has been chosen by an a priori prescription.

However, it is seen that there are still differences between the calculated and the experimental results. In the final set of calculations the dependence of γ on α_w was adjusted to fit the experimental results. The previously chosen values of γ were multiplied by a linear function of $(\alpha_w)^2$. The solid curves on Figs. 1 and 2 which fit the experimental data quite well, where then calculated. The α_w-dependence of γ used for these final calculations is shown as a solid curve in Fig. 4. Note that the same dependence was used for catheters of both materials and all lengths. For the final calculations on the silastic catheters (the solid curve on Fig. 2) the wall constant k was taken as 60% of the measured value. This is believed to be within the errors of the measurement of k and gives improved agreement with experiment. The wall constant for polyethylene catheters was not changed from the measured value.

The calculations reported in this paper were made with the pressure-transducer characteristic $k_t = 3 \times 10^{-10}$, obtained from the manufacturer's specifications. This corresponds to a very small volume displacement over the normal range of pressures. To determine the affect of the pressure transducer, the calculations were repeated with $k_t = 0$ (which is a closed end or perfect pressure transducer). The calculated gains changed by less than 1%.

APPLICATION OF WOMERSLEY'S THEORY TO THE CATHETER

Womersley (2) obtained traveling-wave solutions to a formally linearized system of equations representing fluid flow in a compliant tube. A suitable superposition of solutions has the property that the fluid velocity is zero for all time at some point in space. This point may then be taken as the closed distal end of the catheter. It is then easy to evaluate the pressure amplitudes at the point and at the proximal point a distance L away. Thus, the gain of the catheter can be calculated using Womersley's theory.

The equations for superimposed solutions have been written out by Fry and Greenfield (3). In their equation (4–25) taking $A_1 = A_2$ yields $\bar{w} = 0$ at $z = 0$. Their equation (4–24) may then be used to calculate pressures at $z = 0$ (distal end) and $z = L$ (proximal end).

The gains calculated in this way are shown as a solid curve in Fig. 5 and are seen to be higher than the experimental values. The reason for this discrepancy is not clear. In the first calculations described in the previous section, there was a similar discrepancy with experiment, but this could be removed by a different estimate of the velocity profile. In the case of the calculation using Womersley's theory, the velocity profile is not an unknown function and so cannot be adjusted to remove the discrepancy with experiment.

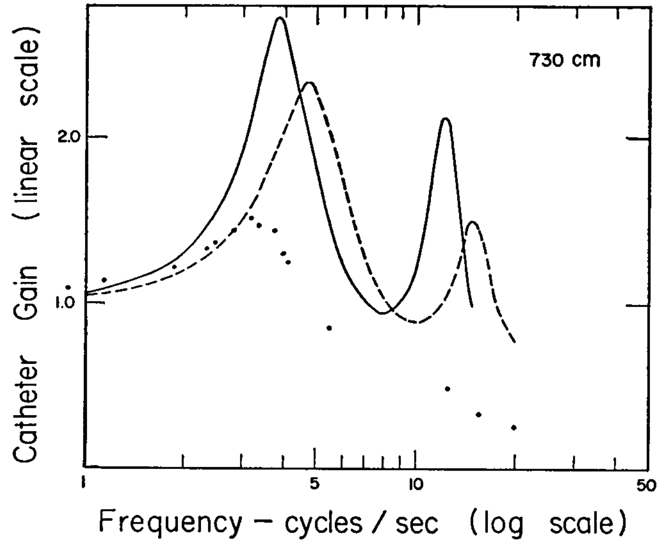

FIGURE 5 Results of applying Womersley's theory to the catheter appear as a solid curve. Results of using Lambossy's friction term are shown as a dashed curve. The points are the experimental values of Fig. 1 ($L = 730$ cm).

There are two possible causes of the difference between experiment and the calculation using Womersley's theory. One is the effect of the nonlinear terms which Womersley drops from the Navier-Stokes equations. The other is the axial motion of the wall, which is permitted in Womersley's model.

APPLICATION OF LAMBOSSY'S FRICTION TERM TO THE CATHETER

The frictional term for a rigid tube was given by Lambossy (4) in a form suitable for numerical calculations. If this friction term is multiplied by $2\pi R$ it can be written in the form

$$2\pi RF = -\rho\gamma U - \rho A(\alpha - 1)\frac{\partial U}{\partial t}$$

where ρ is the density, and γ and α are the terms appearing in the numerical model. Using this form for the frictional term, the dashed curve given in Fig. 5 was obtained. The inclusion of the $\partial U/\partial t$ term gives a slightly higher gain at resonance compared to the gain obtained using the U term alone.

The numerical calculations made in this paper were made at the Common Research Computer Facility of the Texas Medical Center. The facility is supported by grants from the National Institutes of Health and other sources. The authors would like to thank Mr. Robert H. Crane and Mr. Michael B. McGrath for their programming assistance.

Received for publication 25 May 1966.

REFERENCES

1. Barnard, A. C. L., Hunt, W. A., Timlake, W. P., and Varley, E., *Biophysic. J.*, 1966, **6**, 717.
2. Womersley, J. R., An elastic tube theory of pulse transmission and oscillatory flow in mammalian arteries, Wright Air Development Center Technical Report TR 56-614, 1957.
3. Fry, D. L., and Greenfield, J. C., Jr., *in* Pulsatile Blood Flow, (E. O. Attinger, editor), New York, McGraw-Hill Book Company, 1964, 293.
4. Lambossy, P., *Helvetica Physica Acta,* 1953, **25**, 371.